The Six Isomers of the Cyclohexanol Dimer: A Delicate Test for Dispersion Models

The Six Isomers of the Cyclohexanol Dimer: A Delicate Test for Dispersion Models

*Marcos Juanes, Imanol Usabiaga, Iker León, Luca Evangelisti, José A. Fernández, and Alberto Lesarri**

Abstract: *The cyclohexanol homodimer acts as a delicate test model of the role of dispersion forces in intermolecular association. Whereas phenol produces a single dimer, the suppression of π interactions and the larger conformational flexibility in cyclohexanol results in multiple isomerism, with six competing dimers of the free molecule being observed in a supersonic jet expansion. Rotational spectroscopy reveals accurate structural data, specifically the formation of homo- and heterochiral diastereoisomers and the presence of both equatorial and axial forms in the dimers. Four dispersion-corrected density-functional molecular orbital calculations were tested against the experiment, with B3LYP-D3(BJ) offering good structural reproducibility with an Alrich's triple-ζ basis set. However, the prediction of the dimer energetics is largely model-dependent, thus offering a testbed for the validation of dispersion-corrected computational models.*

Chiral recognition is as a pervasive molecular player in biological and supramolecular chemistry, directly influencing ligand binding and macromolecular assembly.[1] Experiments in the gas phase give structural, dynamic, and energetic information on the noncovalent interactions observed in the association of free chiral molecules,[2–4] with the ultimate goal of understanding the molecular basis of enantioselectivity. However, the lack of a general and applicable aggregation model, the multiple intermolecular forces, the variety of interaction energies, the cooperative and competitive effects, and the need for accurate empirical data to validate quantum mechanical models call for additional experiments on chiral recognition between isolated molecules.

Chiral recognition is primarily affected by the stereomutation barriers. Low stereomutation barriers are denoted as transient chirality, and the molecular recognition process, which might involve a structural readaptation, has been categorized as chirality synchronization.[2] Homodimers with transient chirality are interesting because the formation of the cluster quenches the stereomutation, thereby offering the possibility to detect the hetero- and homochiral diastereomeric clusters separately and giving insight into the recognition process.

Torsional chirality has been mostly studied in alcohol dimers, because of the moderately strong O−H···O hydrogen bond and the possibility of using the O-H stretching vibration as a structural probe in IR,[5] Raman,[6] IR/UV,[7,8] or IR/IR/IR[9] spectroscopy. Microwave spectroscopy offers higher (sub-Doppler) resolution, unambiguous structural identification, and general applicability.[4,10] However, the number of rotational studies on transiently chiral dimers is small.[11–19] The analysis of the cyclohexanol dimer explores the balance of intermolecular forces and the differences with phenol aggregation.[20] Our results reveal a rich isomerism, which has led to unexpected questions. In particular, how do noncovalent forces affect isomerism? Can density functional theory (DFT) account for the energetics and structure? And, finally, can you invert a cyclohexanol ring in a jet expansion?

Cyclohexanol offers a variety of structural families, based on *axial* (A)/*equatorial* (E) inverting chair conformations and large-amplitude vibration of the hydroxy group (Figure 1). The most stable equatorial conformer is a fluxional structure that tunnels between two symmetry-equivalent *equatorial-gauche* (EG+ and EG−) isomers, splitting the ground-vibrational state into two torsional-rotation sublevels ($\Delta E_{01} = 52(2)$ GHz).[21] The *equatorial-trans* (ET) conformer

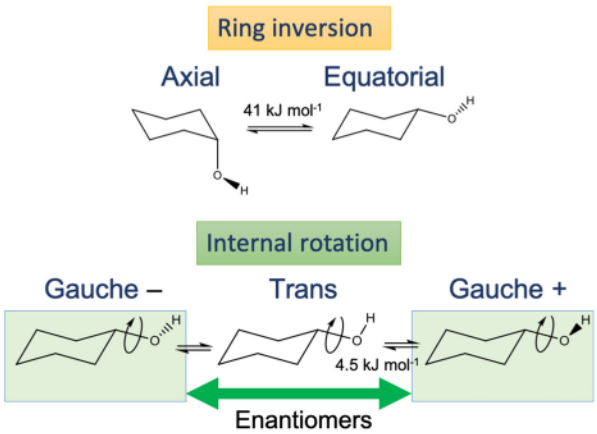

Figure 1. Large-amplitude motions in the cyclohexanol monomer.

[*] M. Juanes, Dr. I. León, Prof. Dr. A. Lesarri
Departamento de Química Física y Química Inorgánica—I.U. CINQUIMA, Universidad de Valladolid
Paseo de Belén, 7, 47011 Valladolid (Spain)
E-mail: alberto.lesarri@uva.es
Dr. I. Usabiaga, Dr. I. León, Prof. Dr. J. A. Fernández
Departamento de Química Física
Universidad del País Vasco, Ap. 644, 48080 Bilbao (Spain)
Dr. I. Usabiaga
Instituto Biofisika (CSIC, UPV/EHU), 48940 Leioa (Spain)
Dr. L. Evangelisti
Dipartimento di Chimica "G. Ciamician"
Università di Bologna, Via Selmi, 2, 40126 Bologna (Italy)

adopts a nondegenerate rigid structure. The *axial* conformers (ca. 2–6 kJ mol^{-1}), previously observed for 1-methylcyclohexanol,[22] were not detected for cyclohexanol.[21] Formation of the cyclohexanol dimer results in the *gauche* stereomutation being broken and the two enantiomers becoming distinguishable, thereby producing distinct diastereoisomers. Assuming that the dimer is primary stabilized by a conventional O−H···O hydrogen bond, the two oxygen lone pairs in the proton acceptor offer six (2 E/A and 3 G+/G−/T) possibilities for each of the six proton donor cases, thus forming 72 isomer families in 36 enantiomeric pairs. However, previous vibrational investigations could only identify a single EG-EG isomer.[9] Recent FTIR and Raman jet spectra have suggested at least four isomers;[23] thus conclusive investigations are necessary.

Cyclohexanol was first probed in a neon jet expansion using broadband chirped-pulsed microwave spectroscopy[24,25] (see the Supporting Information). The spectrum in Figure 2 (see also Figures S1 and S2 in the Supporting Information) is dominated by the monomer, but contains other weak (intensity 5–10%) features from plausible clusters. The spectral assignment started from trial rotational constants and iteratively led to the identification of six isomers of the homodimer (I–VI). The rotational transitions (Tables S1–S6) were fitted to a semirigid-rotor Hamiltonian,[26] with the spectroscopic parameters shown in Table 1. A second experiment in helium did not identify additional species. Experiments with argon showed only isomers II, III, and IV, thus confirming that the global minimum is one of these species as well as the presence of conformational relaxation.[27]

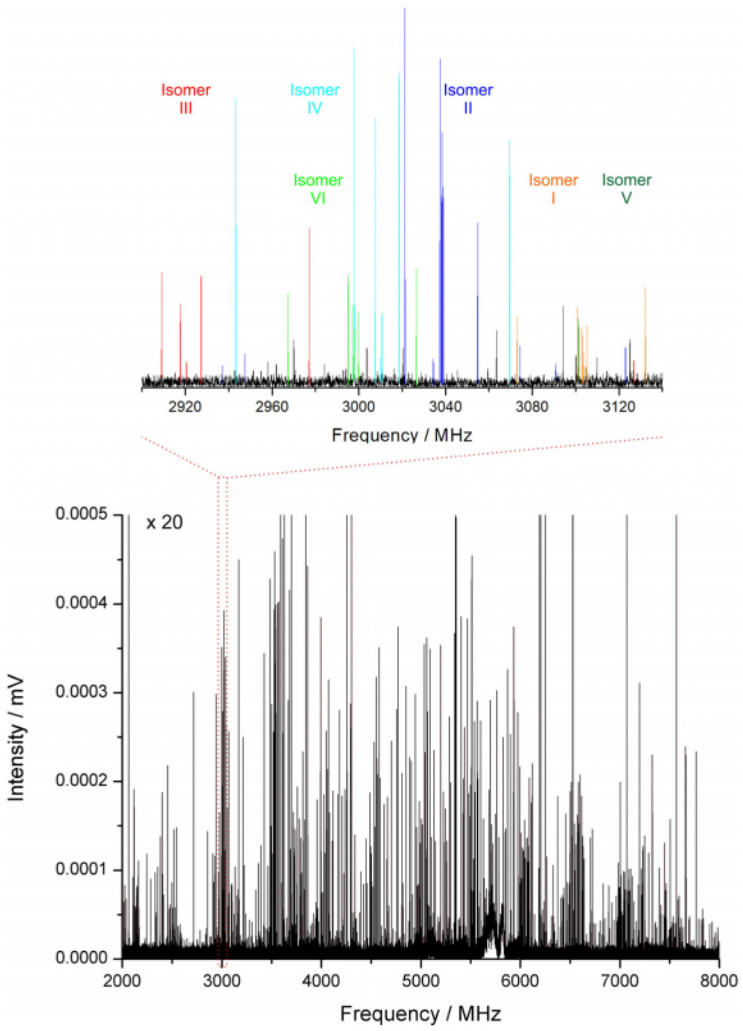

Figure 2. The microwave spectrum of the cyclohexanol dimer and a 240 MHz expansion, showing transitions from six different isomers.

The experiment was rationalized with molecular orbital calculations. The potential energy surface (PES) was, as expected, quite shallow and corrugated, with multiple local minima of low energy, low isomerization barriers, and multiple interconversion paths. Our computational strategy (see the Supporting Information) used molecular mechanics (MM) screening followed by DFT[28] optimizations to probe the maximum conformational space, as in previous experiments.[29] The 60 most stable isomers of the initial 203 MM structures (< 20 kJ mol^{-1}) were reoptimized with three hybrid or meta-GGA functionals, including B3LYP,[30] MN15-L,[31] and M06-2X,[32] using Ahlrichs' polarized triple-zeta basis set def2-TZVP.[33] Minnesota functionals were assumed parametrized for dispersion. B3LYP was supplemented with D3[34] dispersion corrections and Becke–Johnson damping.[35] Finally, the isomers located with each method were reoptimized with the other two functionals. Geometry convergence was very sensitive, with minor changes in the initial geometries resulting in different final structures. Tables S7–S9 summarize data from the conformational search.

All observed isomers could be identified with one of the predicted structures. However, the three DFT methods describe the experiment differently. MN15-L and M06-2X behaved similarly and reproduced the rotational constants with larger relative deviations (ca. 2.0–5.0%). B3LYP-D3(BJ) offered the best agreement, with maximum relative deviations below 3% (i.e. IV and V) and best agreements of 0.1–1.0% (i.e. III and VI). Table S10 compares experiment and theory for B3LYP-D3(BJ). The results support the argument that Minnesota functionals might need corrections for long-range dispersion.[28] Despite the good agreement, both the multiple geometry convergence pathways and the fact that small structural changes (exchange of donor/acceptor or hydroxy internal rotation) may produce similar rotational constants and conformational energies make the structural conclusions model-dependent. Model-dependence was confirmed by an independent conformational search using PW6B95-D3[36,37] and a ωB97X-D[38] reoptimization of the six observed dimers in Table S10.

Isomer identification is shown in Table 1 and Figure 3, with labels indicating the *equatorial/axial* and *gauche/trans* orientations for the proton donor and acceptor, respectively, the (+/−) *gauche* chirality (relative to a $^1C_4$ chair), and the position of the bridging oxygen lone pair (1/2) at the proton

Table 1: Rotational parameters for isomers I–VI of the cyclohexanol dimer.[a]

	Isomer I AT(2)EG−	Isomer II EG−(2)EG−	Isomer III EG−(1)AG−	Isomer IV EG−(1)AG+	Isomer V AG−(1)EG+	Isomer VI EG−(1)EG+
A/ MHz	1218.11(23)[c]	1273.9599(22)	1203.5721(82)	1167.877(41)	1039.694(67)	1311.72(22)
B/ MHz	316.22133(97)	255.99343(18)	303.99025(48)	313.51209(51)	328.52277(90)	254.73673(31)
C/ MHz	304.41165(91)	250.38848(19)	279.76964(43)	288.25106(51)	304.34728(85)	244.86010(34)
D_J/ kHz	0.0583(13)	0.05908(57)	0.06469(69)	0.06942(56)	0.2037(13)	0.06438(54)
D_{JK}/ kHz	−0.1976(88)	−0.4638(99)	−0.2661(34)	−0.2290(26)	−0.475(11)	−0.5107(72)
D_K/ kHz	[0.0]	1.45(34)	[0.0]	[0.0]	[0.0]	[0.0]
d_1/ kHz	−0.0043(19)	[0.0]	−0.01083(87)	−0.01058(97)	−0.0286(20)	[0.0]
N[b]	71	129	101	106	69	100
σ/ kHz	13.0	13.3	10.3	8.3	12.2	13.5

[a] Rotational constants (A, B, C) and Watson's S-reduction centrifugal distortion constants (D_J, D_{JK}, D_K, d_1, d_2 = [0.0]). [b] Number of transitions (N) and root-mean-square (rms) deviation (σ) of the fit. [c] Standard errors in units of the last digit.

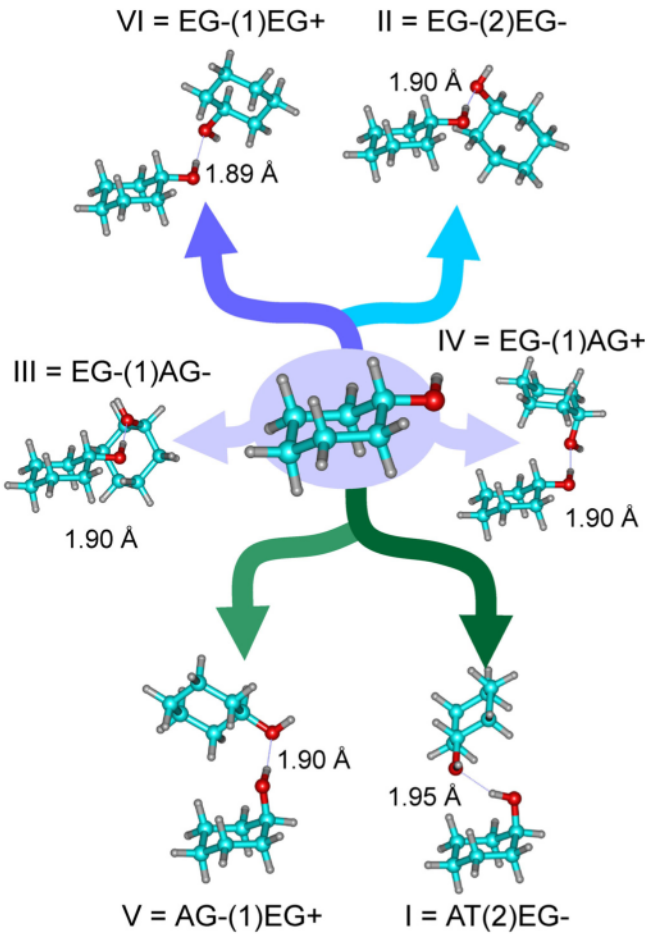

Figure 3. Conformational assignment of the six isomers of the cyclohexanol dimer and hydrogen bond lengths according to B3LYP-D3(BJ)/def2-TZVP.

acceptor. The *equatorial-gauche* system appears in all isomers, as expected from its larger stability in the monomer. However, one of the two monomers occasionally adopts other geometries (see Figures S3–S8 and Tables S11–S16). Specifically, three isomers contain an *axial-gauche* moiety (III = EG−(1)AG−, IV = EG−(1)AG+, V = AG−(1)EG+) and one isomer contains the *axial-trans* orientation (I = AT-(2)EG−). The two remaining isomers are composed exclusively of *equatorial-gauche* forms (II = EG−(2)EG−, VI = EG−(1)EG+). The present computational model and the spectral intensities give population ratios of I/II/III/IV/V/VI = 1.0(4):0.7(4):0.6(3):0.5(2):0.3(1):0.3(1). This calculation is only approximate, as it additionally assumes a linear fast-passage polarization regime proportional to the squared dipole moments and uniform instrumental response.[25] No attempt was made to derive experimental conformational energies, since jet populations are affected by conformational relaxation[27] and initial monomer concentrations.[39]

The presence of *axial* forms is noticeable. Unlike 1-methylcyclohexanol, where the bulkier methyl group stabilizes the *axial* hydroxy group,[22] cyclohexanol has a preference for *equatorial* conformations (Figure S9).[21] To explain the axial forms we compared the *equatorial*-to-*axial* potential barriers both in the monomer and the dimer. The inversion barrier for the cyclohexanol chair was estimated as 47–54 kJ mol^{-1} in a coordinate scan (Figure S10, no transient-state calculation). A similar calculation with the dimer starting from each of the observed geometries and averaging over six inversion paths rendered comparatively similar barriers of 44–51 kJ mol^{-1} (Figure S11). We conclude that there are no plausible ring-inversion paths of reduced energy, so the presence of *axial* forms is due to energetic collisions at the initial stages of the expansion. Collisional stabilization of specific isomers undetected in the monomers has been observed in jets for other clusters.[40–42]

The intermolecular interactions have been mapped using plots of noncovalent interactions (Figures 4 and S12–S17), based on a reduced gradient $S\left(=\frac{1}{2\,(3\pi^2)^{1/3}}\frac{|\nabla\rho|}{\rho^{4/3}}\right)$ of the electron density.[43] All the observed structures exhibit an O−H···O hydrogen bond with predicted distances r_e = 1.891–1.904 Å (B3LYP-D3(BJ)), and longer for the AT proton donor (1.948 Å). In some isomers, additional weak C−H···O hydrogen bonds are apparent (2.65–2.82 Å). In all cases, the two cyclohexyl moieties avoid near-stacking structures. The length of the hydrogen bond is intermediate between that of the phenol dimer[20] (O···H: r_0 = 1.837(23)–1.879(38) Å, r_e = 1.87–89 Å; O···O: r_0 = 2.830(36)–2.833(21) Å) and the water dimer (O···O: r_0 = 2.976 Å, r_e = 2.952 Å). Additional insight into the nature of the noncovalent interactions was obtained by energy decomposition. SAPT2+(3)/aug-cc-pVDZ[44] results (Table S17) for cyclohexanol and six related dimers show that, while the primary interaction is electrostatic (159 % of

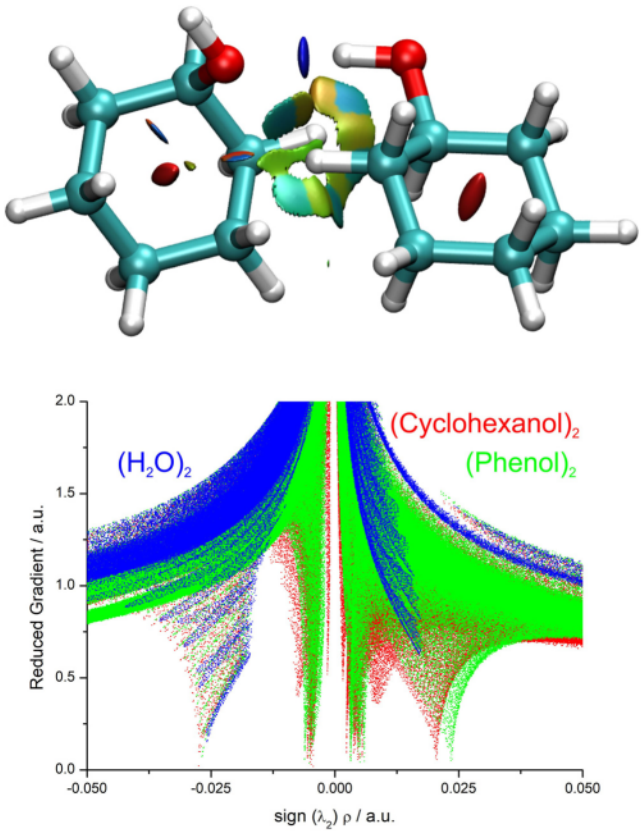

Figure 4. Top: The spatial distribution of the noncovalent interactions in isomer IV of the cyclohexanol dimer, according to a NCIPlot analysis. The O–H···O hydrogen bond (blue) is accompanied by broad weak dispersive interactions (green shades) and repulsive zones (red). Bottom: The reduced electronic density gradient representation for the water (blue), phenol (green), and cyclohexanol dimers (red); see the Supporting Information.

a binding energy of $-29.2\,\mathrm{kJ\,mol^{-1}}$), the dispersion component is very significant (91 %) and similar to that of the phenol dimer (104 %).

In conclusion, we characterized the association between two neutral free molecules of cyclohexanol in a jet expansion. Compared to the phenol dimer,[20] the suppression of π–π or C–H···π stabilization forces and larger flexibility results in multiple isomerism. Stereomutation of the alcohol is quenched in the dimers, so the *gauche* chiral species collapse into different diastereoisomers. However, there is no indication of a dominant stereoselectivity, as both homochiral and heterochiral species are observed in the dimer. In other small alcohol dimers, both homochiral[11,12] and heterochiral[13,14,17] preferences have been observed, thus suggesting sensitive isomerization equilibria on a shallow multiconformational PES.

Competition between multiple low-energy species makes the computational survey difficult. All three DFT methods showed indications of: a) a quite flat potential energy surface, with final structures very dependent of the initial geometry and computational method, b) considerable model changes in the determined isomer energies, and c) deficiencies in assessing the relative energy ordering and global minimum. The dimer DFT energetics were found to be model-dependent and provides an interesting testbed for the predictability of more advanced computational models describing noncovalent interactions. This issue can be related to the most general search of benchmark clusters and appropriate dispersion models within the "DFT zoo", as advocated by Grimme and co-workers.[28] This result shows how the combination of rotational data and computational methods provides a synergistic benefit to characterize weakly bound chirality recognition models in the gas phase.

Acknowledgements

Funding from the Spanish MICINN-FEDER (PGC2018-098561-B-C22) and JCyL (VA056G18) is gratefully acknowledged.

Conflict of interest

The authors declare no conflict of interest.

Keywords: cyclohexanol · hydrogen bonding · jet spectroscopy · molecular recognition · rotational spectroscopy

[1] S. M. Morrow, A. J. Bissette, S. P. Fletcher, *Nat. Nanotechnol.* **2017**, *12*, 410–419.
[2] A. Zehnacker, M. A. Suhm, *Angew. Chem. Int. Ed.* **2008**, *47*, 6970–6992; *Angew. Chem.* **2008**, *120*, 7076–7100.
[3] *Chiral Recognition in the Gas Phase* (Ed.: A. Zehnacker), CRC Press, Boca Raton, FL, **2010**.
[4] M. Juanes, R. T. Saragi, W. Caminati, A. Lesarri, *Chem. Eur. J.* **2019**, *25*, 11402–11411.
[5] T. B. Adler, N. Borho, M. Reiher, M. A. Suhm, *Angew. Chem. Int. Ed.* **2006**, *45*, 3440–3445; *Angew. Chem.* **2006**, *118*, 3518–3523.
[6] T. N. Wassermann, P. Zielke, J. J. Lee, C. Cézard, M. A. Suhm, *J. Phys. Chem. A* **2007**, *111*, 7437–7448.
[7] I. Usabiaga, A. Camiruaga, C. Calabrese, A. Maris, J. A. Fernández, *Chem. Eur. J.* **2019**, *25*, 14230–14236.
[8] A. M. Rijs, J. Oomens, in *Gas-Phase IR Spectrosc. Struct. Biol. Mol.* (Eds.: A. M. Rijs, J. Oomens), Springer International Publishing, Cham, **2015**, pp. 1–42.
[9] I. León, R. Montero, A. Longarte, J. A. Fernández, *J. Chem. Phys.* **2013**, *139*, 174312.
[10] W. Caminati, J.-U. Grabow, in *Frontiers and Advances in Molecular Spectroscopy* (Ed.: J. Laane), Elsevier, Amsterdam, **2018**, pp. 569–598.
[11] J. P. I. Hearn, R. V. Cobley, B. J. Howard, *J. Chem. Phys.* **2005**, *123*, 134324.
[12] D. Loru, I. Peña, M. E. Sanz, *J. Mol. Spectrosc.* **2017**, *335*, 93–101.
[13] M. S. Snow, B. J. Howard, L. Evangelisti, W. Caminati, *J. Phys. Chem. A* **2011**, *115*, 47–51.
[14] A. K. King, B. J. Howard, *Chem. Phys. Lett.* **2001**, *348*, 343–349.
[15] Z. Su, N. Borho, Y. Xu, *J. Am. Chem. Soc.* **2006**, *128*, 17126–17131.
[16] A. Maris, B. M. Giuliano, D. Bonazzi, W. Caminati, *J. Am. Chem. Soc.* **2008**, *130*, 13860–13861.
[17] X. Liu, N. Borho, Y. Xu, *Chem. Eur. J.* **2009**, *15*, 270–277.
[18] J. Thomas, Y. Xu, *J. Phys. Chem. Lett.* **2014**, *5*, 1850–1855.

[19] N. A. Seifert, C. Pérez, J. L. Neill, B. H. Pate, M. Vallejo-López, A. Lesarri, E. J. Cocinero, F. Castaño, *Phys. Chem. Chem. Phys.* **2015**, *17*, 18282 – 18287.
[20] N. A. Seifert, A. L. Steber, J. L. Neill, C. Pérez, D. P. Zaleski, B. H. Pate, A. Lesarri, *Phys. Chem. Chem. Phys.* **2013**, *15*, 11468 – 11477.
[21] M. Juanes, W. Li, L. Spada, L. Evangelisti, A. Lesarri, W. Caminati, *Phys. Chem. Chem. Phys.* **2019**, *21*, 3676 – 3682.
[22] W. Li, L. Spada, L. Evangelisti, W. Caminati, *J. Phys. Chem. A* **2016**, *120*, 4338 – 4342.
[23] B. Hartwig, M. Heger, M. A. Suhm, *Private Communication*, **2020**.
[24] S. T. Shipman, B. H. Pate, in *Handbook of High-Resolution Spectroscopy* (Eds.: F. Merkt, M. Quack), Wiley, New York, **2011**, pp. 801 – 828.
[25] J.-U. Grabow, in *Handbook of High-Resolution Spectroscopy* (Eds.: F. Merkt, M. Quack), Wiley, New York, **2011**, pp. 723 – 799.
[26] J. K. G. Watson, in *Vibrational Spectra and Structure*, *Vol. 6* (Ed.: J. R. Durig), Elsevier, Amsterdam, **1977**, pp. 1 – 89.
[27] P. D. Godfrey, F. M. Rodgers, R. D. Brown, *J. Am. Chem. Soc.* **1997**, *119*, 2232 – 2239.
[28] L. Goerigk, A. Hansen, C. Bauer, S. Ehrlich, A. Najibi, S. Grimme, *Phys. Chem. Chem. Phys.* **2017**, *19*, 32184 – 32215.
[29] M. Juanes, A. Lesarri, R. Pinacho, E. Charro, J. E. Rubio, L. Enríquez, M. Jaraíz, *Chem. Eur. J.* **2018**, *24*, 6564 – 6571.
[30] A. D. Becke, *J. Chem. Phys.* **1993**, *98*, 5648 – 5652.
[31] H. S. Yu, X. He, D. G. Truhlar, *J. Chem. Theory Comput.* **2016**, *12*, 1280 – 1293.
[32] Y. Zhao, D. G. Truhlar, *Theor. Chem. Acc.* **2008**, *120*, 215 – 241.
[33] F. Weigend, R. Ahlrichs, *Phys. Chem. Chem. Phys.* **2005**, *7*, 3297 – 3305.
[34] S. Grimme, J. Antony, S. Ehrlich, H. Krieg, *J. Chem. Phys.* **2010**, *132*, 154104.
[35] S. Grimme, S. Ehrlich, L. Goerigk, *J. Comput. Chem.* **2011**, *32*, 1456 – 1465.
[36] S. Grimme, *Private Communication*, **2020**.
[37] C. Bannwarth, S. Ehlert, S. Grimme, *J. Chem. Theory Comput.* **2019**, *15*, 1652 – 1671.
[38] J. Da Chai, M. Head-Gordon, *Phys. Chem. Chem. Phys.* **2008**, *10*, 6615 – 6620.
[39] W. Caminati, J. C. López, S. Blanco, S. Mata, J. L. Alonso, *Phys. Chem. Chem. Phys.* **2010**, *12*, 10230 – 10234.
[40] J. Thomas, N. A. Seifert, W. Jäger, Y. Xu, *Angew. Chem. Int. Ed.* **2017**, *56*, 6289 – 6293; *Angew. Chem.* **2017**, *129*, 6386 – 6390.
[41] N. A. Seifert, J. Thomas, W. Jäger, Y. Xu, *Phys. Chem. Chem. Phys.* **2018**, *20*, 27630 – 27637.
[42] S. Oswald, N. A. Seifert, F. Bohle, M. Gawrilow, S. Grimme, W. Jäger, Y. Xu, M. A. Suhm, *Angew. Chem. Int. Ed.* **2019**, *58*, 5080 – 5084; *Angew. Chem.* **2019**, *131*, 5134 – 5138.
[43] E. R. Johnson, S. Keinan, P. Mori-Sánchez, J. Contreras-García, A. J. Cohen, W. Yang, *J. Am. Chem. Soc.* **2010**, *132*, 6498 – 6506.
[44] E. G. Hohenstein, C. D. Sherrill, *J. Chem. Phys.* **2010**, *133*, 014101.

Manuscript received: April 7, 2020
Revised manuscript received: May 11, 2020
Accepted manuscript online: May 12, 2020
Version of record online: June 8, 2020